

RSC Advances



This is an *Accepted Manuscript*, which has been through the Royal Society of Chemistry peer review process and has been accepted for publication.

Accepted Manuscripts are published online shortly after acceptance, before technical editing, formatting and proof reading. Using this free service, authors can make their results available to the community, in citable form, before we publish the edited article. This *Accepted Manuscript* will be replaced by the edited, formatted and paginated article as soon as this is available.

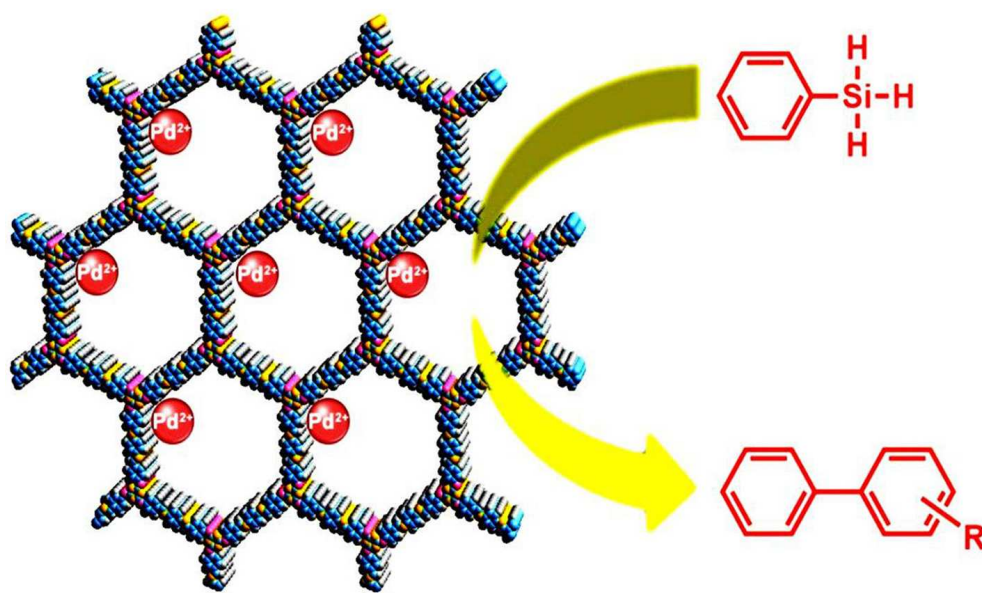
You can find more information about *Accepted Manuscripts* in the [Information for Authors](#).

Please note that technical editing may introduce minor changes to the text and/or graphics, which may alter content. The journal's standard [Terms & Conditions](#) and the [Ethical guidelines](#) still apply. In no event shall the Royal Society of Chemistry be held responsible for any errors or omissions in this *Accepted Manuscript* or any consequences arising from the use of any information it contains.

A triazine-based covalent organic framework-palladium hybrid for one-pot silicon-based cross-coupling of silanes and aryl iodides

Sha Lin,^a Yuxia Hou,^b Xiao Deng,^a Haoliang Wang,^a Shuzhuang Sun^a and Xiaomei Zhang^{*a}

A palladium/COF hybrid material could efficiently catalyze the silicon-based one-pot cross-coupling reaction of silanes and aryl iodides with excellent selectivity.



ARTICLE

A triazine-based covalent organic framework-palladium hybrid for one-pot silicon-based cross-coupling of silanes and aryl iodides

Cite this: DOI: 10.1039/x0xx00000x

Received 00th January 2012,
Accepted 00th January 2012

DOI: 10.1039/x0xx00000x

www.rsc.org/Sha Lin,^a Yuxia Hou,^b Xiao Deng,^a Haoliang Wang,^a Shuzhuang Sun^a and Xiaomei Zhang*^a

A triazine-based covalent organic framework (**COF-SDU1**) was synthesized through a facile solvothermal condition and characterized by IR, solid state ¹³C NMR, XRD, elemental analysis and BET. By a simple solution infiltration method, Pd(II) species were successfully immobilized into **COF-SDU1** due to its two-dimensional eclipsed layer-sheet structure and nitrogen-rich content. High-resolution TEM images showed the uniform loading of the Pd species into the **COF-SDU1** matrix. By using this hybrid material, **Pd(II)/COF-SDU1**, as a sustainable and green catalyst, a one-pot cross-coupling of silanes and aryl iodides was realized with high selectivity. The catalyst can be easily recovered by a simple separation process and recycled for several times without obvious loss of activity and selectivity.

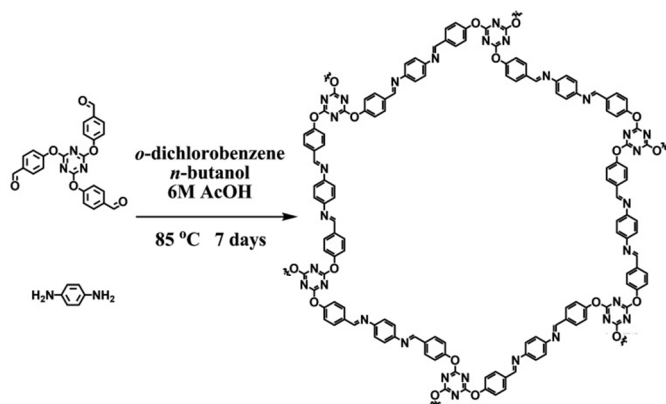
Introduction

The carbon-carbon cross-coupling reactions are one of the most crucial transformations in synthetic chemistry due to their extensive application in forming novel organic compounds.¹ Among them, the silicon-based cross-coupling reaction is an emerging interesting method based on its non-toxicity, high chemical stability and broad availability.² To date, many types of silicon coupling reagents have been developed, such as organo(alkoxy)silanes and organosilanols.³ However, the synthesis of these silicon coupling reagents often need the complicated and toxic raw materials. Meanwhile, the separation and the purification are difficult because some of them are easy to dimerize.⁴ In recent years, oxidation of organosilanes to fabricate silicon coupling reagents catalyzed by transition metal has been rapidly developed.⁵ This method was more green and facile over the above conventional routes. Because the oxides in these reactions are water or alcohols and the only by-product is H₂. Progressively, if the synthesis of silicon coupling reagents and the following cross-coupling could combine in one-pot, separation of intermediates would be avoided and the reaction would be green, dexterous and environmentally friendly. Rare related work has been investigated so far. Very recently, our group firstly realized the silicon-based one-pot cross-coupling reaction by using ordinary organosilanes as starting materials catalyzed by nanoporous Pd.⁶ Although excellent yield was reached, homocoupling side product of aryl iodides inevitably existed. Furthermore, the preparation of nanoporous Pd catalyst

is complicated. To solve these problems and further optimize silicon-based cross-coupling reaction with high yield and selectivity, design and fabrication of highly effective and sustainable catalysts are of great importance.

Covalent organic frameworks (COFs),⁷ as the emerging stable and porous materials, have attracted increasing interests in the past ten years due to their various applications in gas storage,⁸ chemical sensing,⁹ and catalytic supports.¹⁰ The fascinating features of COFs, such as high surface area, porosity and structural tunability, make them to be the brilliant candidates as versatile and efficient supports for various catalytically active metals. In this view, as COFs were synthesized by strong covalent bonds and elaborately designed building blocks, their chemical functionalities and structural properties could be tuned by appropriate choice of the starting building block and modification of the synthetic process. Therefore, COFs would be more suitable for anchoring and mono-dispersing metal ion due to their effective interplay between metal ion and the elaborately designed functional groups. In fact, a few cases of COF/metal hybrids have exhibited excellent catalytic activity in organic reactions, such as Suzuki coupling,^{10a,11} glycerol oxidation,¹² nitro reduction,¹³ Heck-Sonogashira coupling^{10c} etc. in the last few years. Inspired by the remarkably catalytic performances of the emerging COF/metal hybrids, seeking novel COF/metal hybrids catalysts and expanding their catalytic applications in more extensive reaction types have received more and more attention.

Previous investigations have revealed that the introduction of nitrogen functionalities on the supports could increase the dispersion and stability of some metal nanoparticles. In this respect, nitrogen-modified activated carbons as supports for platinum and palladium have attracted great interest in the liquid-phase oxidation of alcohols.¹⁴ For COFs materials, Wang,^{10a} Banerjee,^{10b,c} Prati,¹² Schüth^{10e} et al. had also demonstrated that imine-based and triazine-based COFs could immobilize and disperse palladium, gold, and platinum well. And these COF/metal hybrids exhibited increasing catalytic activity in organic reactions. Based on these considerations, in present work, we design and synthesize a nitrogen-rich triazine building block tri-(4-formacylphenoxy)-1,3,5-triazine (trif) (Scheme 1). By a facile solvothermal reaction between trif and *p*-phenylenediamine, a novel COF material (**COF-SDU1**) containing both imine and triazine functional groups was obtained. This material can sturdily stabilize and regularly mono-disperse the palladium species due to **COF-SDU1**'s two-dimensional eclipsed layer-sheet structure and nitrogen-rich content. The **Pd(II)/COF-SDU1**, as a sustainable and green catalyst, exhibits excellent catalytic activity and selectivity towards the silicon-based one-pot cross-coupling reaction of silanes and aryl iodide. In addition, the catalyst can be reused several times without obvious metal leaching, sintering behaviors and evident loss of catalytic activity.



Scheme 1. The preparation of **COF-SDU1** by the condensation reaction between trif and *p*-phenylenediamine.

Experimental Section

General

Column chromatography was carried out on silica gel (Merck, Kieselgel 60, 200-300 mesh) with the indicated eluents. *p*-hydroxybenzaldehyde and *p*-phenylenediamine were obtained from Sinopharm Chemical Reagent Limited Company. Tri-(4-formacylphenoxy)-1,3,5-triazine (trif) was prepared according to the published procedure.¹⁵ All other reagents and solvents were of analytical grade and used as received without further purification.

Measurements

¹H NMR spectra were recorded on a Bruker DPX 400 spectrometer. Spectra were referenced internally using the residual solvent resonances relative to SiMe₄. Solid-state NMR experiments were performed on Bruker AVANCE III 600 spectrometer at a resonance frequency of 150.9 MHz. ¹³C CP/MAS NMR spectra were recorded using a 4 mm MAS probe and a spinning rate of 8 kHz. A contact time of 2 ms, a recycle delay of 5 s, and 4000 accumulations were used for the ¹H-¹³C CP/MAS measurement. Fourier transform infrared spectra (FT-IR) were recorded in KBr pellets with 2 cm⁻¹ resolution using an α ALPHA-T spectrometer. MALDI-TOF mass spectra were taken on a Bruker BIFLEX III ultra-high resolution Fourier transform ion cyclotron resonance (FT-ICR) mass spectrometer with α -cyano-4-hydroxycinnamic acid as matrix. Elemental analyses were performed on an Elementar Vavio El III elemental analyzer. Powder X-ray diffraction (PXRD) measurements were carried out on a Rigaku D/mas- γ B X-ray diffractometer with a Cu-K α sealed tube ($\lambda=1.5406$ Å) at 293K. High-resolution transmission electron microscopy (HR-TEM) images were measured on a JEOL JEM-2100 electron microscope operated at 200 kV. Scanning electron microscopy (SEM) images were obtained using a JEOL JSM-6700F field-emission scanning electron microscopy. For TEM imaging, a drop of freshly prepared sample solution was cast onto a carbon copper grid. For SEM imaging, C (1-2 nm) was sputtered onto the grids to prevent charging effects and to improve the image clarity. The Pd contents of the COF samples were determined by inductively coupled plasma atomic emission spectroscopy (ICP-AES) analysis with an IRIS Intrepid II XRP instrument. N₂ adsorption-desorption isotherms were measured on an ASAP 2020 (V4.01G) apparatus at 77.3 K and the surface areas of the **COF-SDU1** and **Pd(II)/COF-SDU1** were calculated by both the Brunauer–Emmett–Teller (BET) and Langmuir method. X-ray photoelectron spectroscopy (XPS) was carried out on PHI 5300 ESCA System (Perkin-Elmer, USA). The excitation source is Al K α radiation. AA stacking and AB stacking Molecular modelings and Pawley refinement of the **COF-SDU1** were carried out at the level of PBE-D(Grimme)/DN(4.4) in DMol³ software.

Preparation of COF-SDU1

A mixture of trif (178 mg, 0.4 mmol) and *p*-phenylenediamine (65 mg, 0.6 mmol) in *o*-dichlorobenzene/*n*-butanol/6M AcOH (5/5/1 by vol.; 16.5 mL) was sonicated at room temperature for 0.5 h. Then, the mixture was sealed in a 25-mL Teflon-lined stainless steel container and heated at 85 °C for 7 days. After the temperature of container cooled down to room temperature, a grayish yellow solid was found. This solid was isolated by centrifugation and washed with ethyl acetate, tetrahydrofuran (THF), acetone and chloroform to remove the trapped guest molecules, such as unreacted starting materials, then dried at 70 °C under vacuum for 12 h to yield **COF-SDU1** as a grayish yellow powder (150 mg, yield 65 %); Found: C, 66.21; H, 3.307; N, 17.37. Calc. for (C₁₁H₇ON₂)_n: C, 72.13; H, 3.82; N,

15.30%; IR (powder, cm^{-1}): 3405, 1695, 1620, 1565, 1504, 1365, 1206, 1161, 840, 809; ^{13}C CP/MAS NMR (ppm): 173, 165, 154, 149, 135, 130, 122.

Preparation of Pd(II)/COF-SDU1

$\text{Pd}(\text{OAc})_2$ (15 mg, 0.067 mmol) and **COF-SDU1** (100 mg) were dissolved in 10 mL of dichloromethane. The mixture was kept stirring at room temperature for 24 h. The resulting solid was isolated by centrifugation, washed with dichloromethane, and then dried at 70 °C under vacuum for 12 h to obtain **Pd(II)/COF-SDU1** as a grayish yellow powder (110.8 mg, 89 % yield). The Pd content was 4.5 % as determined by ICP-AES; Found: C, 62.55; H, 3.37; N, 15.79. Calcd for $0.049\text{nPd}(\text{OAc})_2@(\text{C}_{11}\text{H}_7\text{ON}_2)_n$: C, 68.04; H, 3.61; N, 14.43%; IR (powder, cm^{-1}) 3405, 2872, 1698, 1620, 1565, 1502, 1363, 1206, 1161, 841, 809, 619; ^{13}C CP/MAS NMR (ppm) 180, 173, 165, 154, 149, 135, 130, 122, 22.

Silicon-based one-pot cross-coupling reaction

Pd(II)/COF-SDU1 (20 mg) and 0.2 mL of methanol were added into 2 mL of THF solvent at room temperature. Then phenylsilane (108 mg, 1 mmol) was added into this mixture. After no obvious bubbles emerging, iodobenzene derivatives (1.1 mmol) and tetrabutylammonium fluoride (TBAF 3 mmol) were added into the system without changing the reaction vessel and then the reaction temperature was elevated to 80 °C. After the reaction was completed, the mixture was cooled to room temperature, filtered and washed with THF. Then the filtrate was concentrated under vacuum. The residue was purified by silica gel chromatography with the appointed solvent as eluent.

Results and Discussion

Synthesis of COF-SDU1 and Pd(II)/COF-SDU1

COF-SDU1 was synthesized in a good yield under solvothermal condition through the condensation of trif and *p*-phenylenediamine in *o*-dichlorobenzene/*n*-butanol/6M AcOH (5/5/1, volume ratio) at 85 °C for 7 days (Scheme 1). **Pd(II)/COF-SDU1** was prepared by coordinating **COF-SDU1** with $\text{Pd}(\text{OAc})_2$ in dichloromethane at room temperature for 24 h. Both **COF-SDU1** and **Pd(II)/COF-SDU1** are insoluble in water and some polar organic solvents such as THF, acetone and chloroform. The thermal stability of **COF-SDU1** and **Pd(II)/COF-SDU1** was monitored by thermogravimetric analysis (TGA). Under nitrogen conditions, **COF-SDU1** displayed great thermal stability and can be stable up to 450 °C. After being coordinated with $\text{Pd}(\text{OAc})_2$, **Pd(II)/COF-SDU1** still remained high thermal stability. The degradation of this material started at approximately 250 °C (ESI, Fig. S1†). As the temperature of most liquid reaction is below 250 °C, the higher thermal stability would endow **Pd(II)/COF-SDU1** more potential application in liquid phase reactions, even in gas phase reactions.

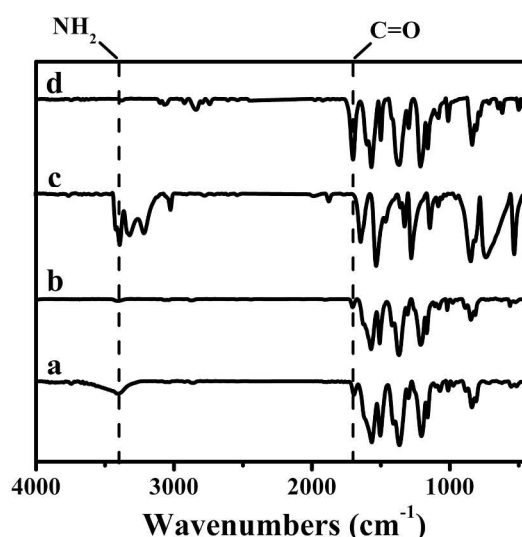


Fig. 1. FT-IR spectra of (a) **COF-SDU1**, (b) **Pd(II)/COF-SDU1**, (c) *p*-phenylenediamine and (d) tri(4-formacylphenoxy)-1,3,5-triazine (trif) in the region of 500-2000 cm^{-1} with 2 cm^{-1} resolution.

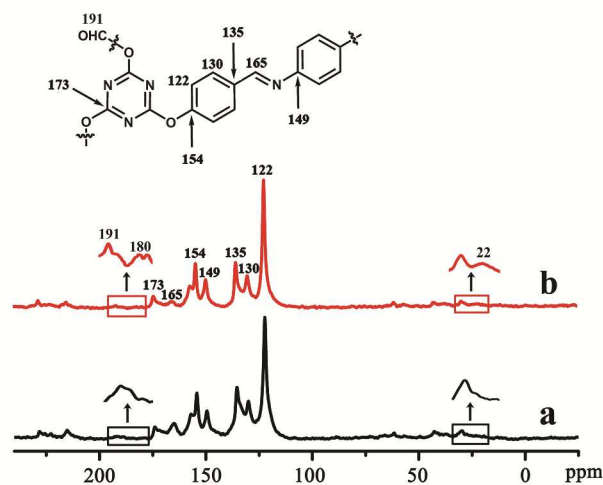


Fig. 2. ^{13}C CP/MAS NMR spectra of (a) **COF-SDU1** and (b) **Pd(II)/COF-SDU1**.

Fourier transform infrared (FT-IR) and ^{13}C CP/MAS NMR spectra

The successful formation of the COFs was assessed by Fourier transform infrared (FT-IR) and ^{13}C CP/MAS NMR spectroscopies. As showed in the FT-IR spectra of the raw materials, the carbonyl stretching band of trif (Fig. 1c) and N-H stretching band of *p*-phenylenediamine (Fig. 1d) were appeared at 1701 and 3377 cm^{-1} respectively. Compared with these starting materials, the clearly weakening absorption bonds for C=O and N-H and the appearance of a new stretching vibration band at 1620 cm^{-1} attributing to the C=N bond were observed in the FT-IR spectra of **COF-SDU1** (Fig. 1a), clearly indicating the successful fabrication of the COFs material. Meantime, the ^{13}C CP/MAS NMR spectrum provided further confirmation for

the formation of imine bonds in the as-synthesized COFs. As showed in Fig. 2a, a characteristic resonance signal at 165 ppm, which was assigned to the C=N bond, was exhibited in the as-synthesized COFs. Furthermore, the strong resonance signals of C=O bond at 191 ppm displayed in the ^{13}C NMR spectrum of trif (ESI, Fig. S2 \dagger) was strongly attenuated. However, the other resonance signals appeared in the ^{13}C NMR spectrum of trif was also existed in the ^{13}C CP/MAS NMR spectrum of **COF-SDU1**.

Similar with **COF-SDU1**, FT-IR and ^{13}C CP/MAS NMR spectra of **Pd(II)/COF-SDU1** exhibited almost identical absorption and resonance peaks with **COF-SDU1** (Fig. 1b and 2b). This result clearly indicated that the crystal structure of **COF-SDU1** was well preserved after the coordination with Pd^{2+} . In addition, in the ^{13}C CP/MAS NMR spectrum of **Pd(II)/COF-SDU1**, two additional minor resonance signals were also observed at ~ 180 and 22 ppm, respectively. According to Wang's previous work,^{10a} these two signals were assigned to the carbonyl and methyl groups of the incorporated $\text{Pd}(\text{OAc})_2$, further implying the effective coordination of Pd^{2+} with **COF-SDU1** materials. Further evidences for this point were also revealed by the PXRD, SEM and TEM results, as detailed below.

X-ray photoelectron spectra (XPS) analysis

To confirm the incorporation of palladium within **COF-SDU1**, X-ray photoelectron spectroscopy (XPS) was employed to detect the Pd ions circumstance. The XPS spectra of $\text{Pd}(\text{OAc})_2$ and **Pd(II)/COF-SDU1** (ESI, Fig. S3 \dagger), indicated that both compounds show typical signals for the Pd^{2+} ion. The strong absorption peak at 338.7 and the weak absorption peak at 344.3 for $\text{Pd}(\text{OAc})_2$ attributed to the $\text{Pd}^{2+}_{3d5/2}$ and $\text{Pd}^{2+}_{3d3/2}$, respectively.¹⁶ In the comparison with the XPS spectrum of $\text{Pd}(\text{OAc})_2$, the Pd^{2+} signals in the XPS spectrum of **Pd(II)/COF-SDU1** take obvious shift to the lower bonding energy direction, implying the stronger coordination of $\text{Pd}(\text{OAc})_2$ with the imine and triazine groups of **COF-SDU1**.^{10a}

Powder X-ray diffraction patterns of **COF-SDU1** and **Pd/COF-SDU1**

Powder X-ray diffraction (PXRD) analysis was used to determine the crystalline structure of **COF-SDU1** and **Pd(II)/COF-SDU1**. Fig. 3A showed the both experimental and simulated PXRD patterns of as-synthesized COF materials. The PXRD diagram of **COF-SDU1** exhibited one intense and three weak peaks at $2\theta = 2.71^\circ$ (corresponding to 3.26 nm), 4.69° (1.88 nm), 5.41° (1.63 nm) and 7.27° (1.22 nm) respectively at the low angle range, which are ascribed to the refractions from the (100), (110), (200), and (210) planes, indicating the long-rang molecular ordering of **COF-SDU1** along these planes. When Pd(II) species was incorporated into **COF-SDU1**, a well maintained PXRD diagram of **Pd(II)/COF-SDU1** with that of **COF-SDU1** was observed. No other diffraction peaks attributed to the Pd(II) species can be found, implying the high dispersion of Pd(II) on **COF-SDU1** materials. Obviously, the

highly dispersed Pd(II) species on **COF-SDU1** did not damage the crystallinity of **COF-SDU1** and the integrity of **COF-SDU1** structure was retained. Next, *Materials Studio software package* was used to elucidate the lattice packing of **COF-SDU1**. Two probable structures, namely a fully eclipsed model with an AA stacking sequence (Fig. 3B) and a staggered model with an AB stacking sequence (Fig. 3C), were simulated.¹⁷ Simulations of AA stacking sequence used *P1* space group with $a = 39.694 \text{ \AA}$, $b = 39.474 \text{ \AA}$, $c = 4.838 \text{ \AA}$ and $\alpha = \beta = 90^\circ\text{C}$, $\gamma = 120^\circ\text{C}$. As can be found in Fig. 3A, the peak positions and relative intensities of AA stacking model was in good accordance with that of the experimentally observed one. While the PXRD pattern of AB staggered stacking mode exhibited a largely deviation from that of the experimentally observed profile. From these results, it can be speculated that **COF-SDU1** was composed of hexagonal layers, stacking along the 001 plane.

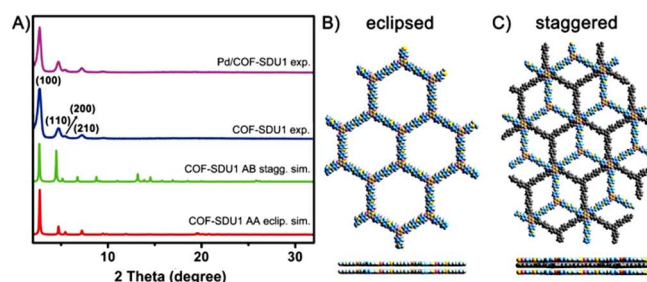


Fig. 3. (A) Experimental PXRD patterns of **COF-SDU1** and **Pd(II)/COF-SDU1** together with the simulated patterns according to AA and AB stacking models. (B) Views of the AA stacking structure along c and b axes. (C) Views of the AB stacking structure along c and b axes.

Morphology of the COFs materials

The morphological and structural features of the as-synthesized both COFs were examined by scanning electron microscopy (SEM) and transmission electron microscopy (TEM). Samples were prepared by casting a drop of sample solution onto a carbon-coated grid. As could be seen from the panoramic SEM image of **COF-SDU1** (Fig. 4A), the sample was mainly composed of numerous uniform spherical clusters of about 1-2 μm in diameter. A close observation (Fig. 4B) revealed that each of the individual clusters was stacked by a large amount of small and dense flake with diameter of 70-90 nm. As results, the surface of **COF-SDU1** was rather rough and rugged, which would be favor of catalytic applications. The corresponding TEM image of **COF-SDU1** (Fig. 4C) indicated that the material was formed by a crowd of homogeneous small flakes within tens of nanometers range, consistent with the SEM results. In the high-resolution transmission electron microscopy (HR-TEM) image of the **COF-SDU1** (Fig. 4D), the lattice fringes could also be observed, clearly implying the highly ordered crystalline structure of the as-synthesized **COF-SDU1**. In the SEM and TEM images of **Pd(II)/COF-SDU1**, it can be seen that the morphology of **Pd(II)/COF-SDU1** was similar with

COF-SDU1 (Fig. 5). Further observation of the high resolution TEM image revealed that the surface of the spherical clusters was covered with the 3–4 nm sized black dots attributed to Pd(0) nanoparticles. However, from the results shown in XPS analysis, the oxidation state of the palladium incorporated into the COF-SDU1 matrix is +2. This may be a consequence of the high energy electron beam during TEM analyses. According to previous research,^{10a,c,18} the loaded Pd²⁺ would get agglomerated first then further reduced spontaneously from Pd(II) to Pd(0) under the action of electron beam during TEM analyses.

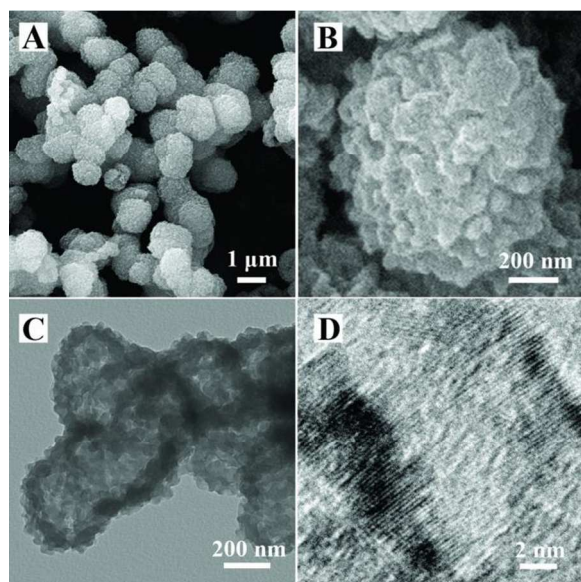


Fig. 4. (A) SEM, (B) amplifying SEM, (C) TEM and (D) high-resolution TEM images of **COF-SDU1**.

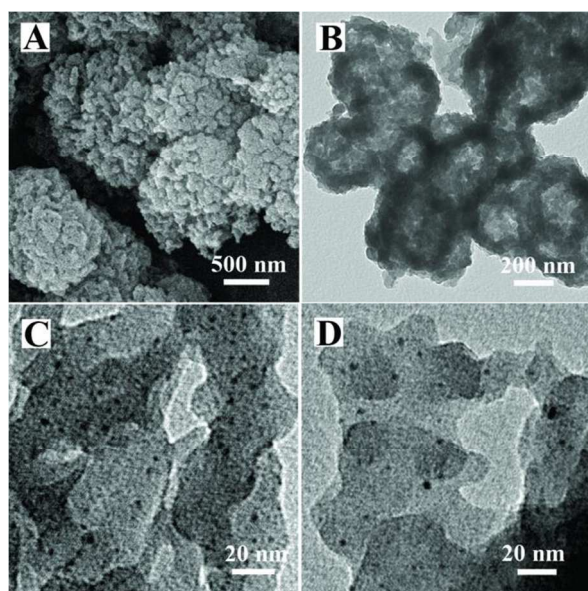


Fig. 5. (A) SEM, (B) amplifying SEM, and high-resolution TEM images of **Pd(II)/COF-SDU1** (C) before and (D) after reused for three times.

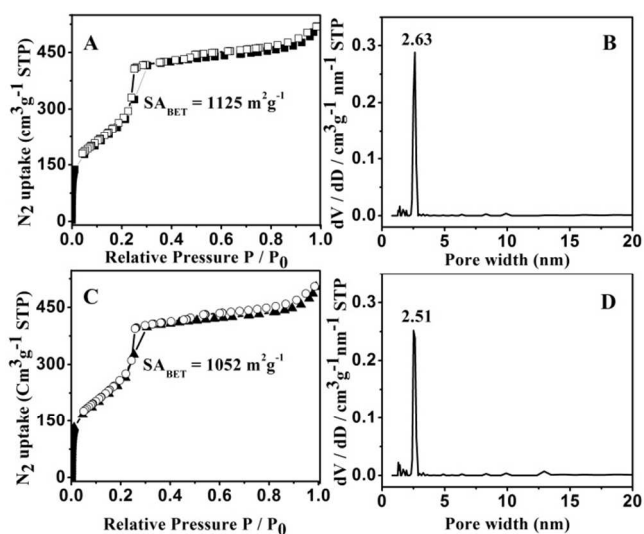


Fig. 6. Nitrogen adsorption- desorption isotherms of (A) **COF-SDU1** and (C) **Pd(II)/COF-SDU1**. Pore-size distribution of (B) **COF-SDU1** and (D) **Pd(II)/COF-SDU1** from nonlocal density functional theory.

Brunauer–Emmett–Teller (BET) surface area

In order to characterize the porosity parameters of **COF-SDU1** and **Pd(II)/COF-SDU1**, the nitrogen adsorption isotherm were measured at 77.3 K. As showed in Fig. 6A, **COF-SDU1** displayed a sharp uptake below $P/P_0 = 0.01$ and a very well-defined jump between $P/P_0 = 0.04 - 0.25$ was also observed, indicating the high crystallinity of the porous system.¹⁹ This profile is assigned to a type IV isotherm, which is characteristic of mesoporous nature of the material. The Brunauer–Emmett–Teller (BET) surface area and Langmuir surface area of **COF-SDU1** were calculated to be 1125 and 3545 m^2g^{-1} , respectively, which is much higher than that of the analogous COFs materials reported previously, such as CTF-1 (791 m^2g^{-1}).²⁰ The total pore volume and pore size distribution were calculated by using the nonlocal density functional theory (NLDFT). The total pore volume was estimated to be 1.20 cm^3g^{-1} at $P/P_0 = 0.98$. The average pore size was mainly centered at around 2.63 nm except a few minor peaks appeared at some smaller pore width range. This result was slight smaller than that of the PXRD and theoretically predicted value (3.2 nm), which may arise from the imperfect solid-state stacking of the eclipsed 2D sheets that cannot be identified by PXRD studies as reported for many 2D COFs and predicated by theoretical studies.^{8c,21} The nitrogen adsorption isotherm of **Pd(II)/COF-SDU1** also possessed a type IV isotherm (Fig. 6C). The total pore volume and pore size distribution calculated by NLDFT were 1.16 cm^3g^{-1} at $P/P_0 = 0.98$ and 2.51 nm, respectively. In comparison with **COF-SDU1**, the pore size of **Pd(II)/COF-SDU1** was nearly parallel to **COF-SDU1**, which indicated that the incorporation of Pd²⁺ did not disturb the internal matrix of **COF-SDU1**. According to the previous investigates, when metal ions or particles were incorporated into the COFs

materials, notable decrease of the BET surface was appeared while the pristine COF materials were maintained.¹⁰ However, in our present case, it is amazing that the BET surface area and Langmuir surface area of **Pd(II)/COF-SDU1** were calculated to be 1052 and 3327 m² g⁻¹, respectively, very closer to that of **COF-SDU1**. The almost unchanged high BET surface would undoubtedly benefit the catalytic performance of **Pd(II)/COF-SDU1**.

Catalytic activity measurement

The catalytic activity of **Pd(II)/COF-SDU1** toward one-pot silicon-based cross-coupling reaction of silanes and aryl halides was accessed. To realize this reaction, oxidation of organosilanes to organo(alkoxy)silanes or organosilanols in good yield and then effectively cross-couples between the organo(alkoxy)silanes or organosilanols with aryl halides are necessary. Therefore, **Pd(II)/COF-SDU1**'s activity towards oxidation of organosilanes to organo(alkoxy)silanes or organosilanols was studied firstly. The reaction was tested in THF solution (2 mL) at room temperature with phenylsilane (1 mmol), water (0.2 mL) and **Pd(II)/COF-SDU1** (20 mg, the mole ratio of Pd species versus phenylsilane was 0.0085). After 2 h, phenylsilanetriol (**1a**) was obtained with 97.8% yield (ESI, Table S1,† entry 1). Similar with water, when methanol or ethanol was used as oxide, the corresponding organo(alkoxy)silanes was also obtained in high yield, (ESI, Table S1,† entries 4-5). Then different substrates were explored. Aromatic organosilanes, no matter containing one, two or three H, could be activated to corresponding organo(alkoxy)silanes or organosilanols within 2-3 h with almost equivalent yield (ESI, Table S1,† entries 1-3), indicating the high activity of **Pd(II)/COF-SDU1** toward the oxidation of organosilanes.

Next, we tested the **Pd(II)/COF-SDU1**'s activity towards silicon-based cross-coupling reaction of the organo(alkoxy)silanes or organosilanols with aryl iodides. Considering the follow-up one-pot reaction, equivalent amount of the catalyst was used. The experiment was carried out firstly with phenyltrimethoxysilane (**1d**) (1mmol), 4-iodotoluene (1.1 mmol), TBAF (3 mmol) at 80 °C in THF (2 mL). After 7 h, 4-methylbiphenyl as the cross-coupling product was obtained (97.8% yield, ESI, Table S2†). On the other hand, no coupling product was obtained in the absence of **Pd(II)/COF-SDU1**, indicating that the reaction was catalyzed by **Pd(II)/COF-SDU1**. Similar with **1d**, other organo(alkoxy)silanes or organosilanols can also be effectively converted into 4-methylbiphenyl (ESI, Table S2†). Moreover, no homo-coupling byproduct was detected. These results implied the high catalytic activity of **Pd(II)/COF-SDU1** for this type of cross-coupling reaction.

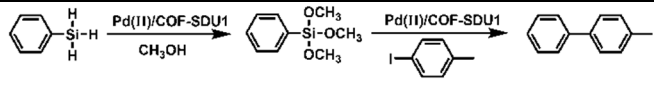
Based on the above experimental observations, **Pd(II)/COF-SDU1** is active for organosilane oxidation as well as silicon-based cross-coupling reaction, individually. Hence, we investigated one-pot silicon-based cross-coupling reaction of

silanes and aryl iodides catalyzed by **Pd(II)/COF-SDU1**. According to the previous research, Si-OH bonds in organosilanols could easily dimerize,²² which was negative to the following no-isolated continuous reaction. Therefore organo(alkoxy)silanes were more suitable as coupling partner. We finally chose methanol instead of water as oxidant to avoid the generation of organosilanols intermediate. The representative reaction conditions were methanol (5 mmol), phenylsilane (1 mmol), 4-iodotoluene (1.1 mmol), TBAF (3 mmol), **Pd(II)/COF-SDU1** (20 mg) and THF (2 mL). After methanol (5 mmol), phenylsilane (1 mmol) and **Pd(II)/COF-SDU1** (20 mg) were reacted in THF at room temperature for 3 h, 4-iodotoluene (1.1 mmol) and TBAF (3 mmol) were added into this mixture. Then the system was heated up to 80 °C. After 7 h, the corresponding cross-coupling product 4-methylbiphenyl (**2a**) was obtained in 96.5 % separated yield (Table 1, entry 1).

We also used nanoporous Pd (np-Pd) and commercial available Pd/C to comparatively test this reaction. The np-Pd was prepared from the reported method,⁵ and the Pd/C (5% Pd) was purchased from Aladdin Industrial Corporation. When using the same condition, especially the same equivalent of 4-iodotoluene (1.1 mmol), the yield of np-Pd was only 50% due to the formation of homo-coupling by-products. Higher yield (91%) was obtained when we increased the dosage of 4-iodotoluene (1.5 mmol). As for Pd/C, 93% yield was obtained under the same condition and a small number of homo-coupling by-products were also detected. However, it was hard to realize the good reusability of Pd/C because of the leaching problem. When Pd/C was reused for the second time, 70% cross-coupling product was obtained.

To evaluate the stability and reusability of **Pd(II)/COF-SDU1**, the recycled and leaching experiments were performed. For leaching, when the reaction was finished, **Pd(II)/COF-SDU1** was filtered from the solution. Then the filtrate was analyzed by inductively coupled plasma atomic emission spectroscopy (ICP-AES). Results showed that the leaching of palladium was lower than the detection limits (<0.02 ppm), indicating the heterogeneity of **Pd(II)/COF-SDU1** catalyst. Owing to the insolubility of **Pd(II)/COF-SDU1** in most of organic solvent, the catalyst can be separated easily by simple filtration. The recovered catalyst was washed with THF and methanol and then reused without further treatment. No significant loss of the catalytic activity was observed (Table 1, entries 2-4) after **Pd(II)/COF-SDU1** was reused for additional three times. The stability of the catalyst after catalytic cycles was further confirmed by comparing the TEM images of the catalyst after catalytic runs with the fresh prepared one. As shown in Fig. 6D, no obvious aggregates and change in the morphology and feature dimensions of the Pd species were observed. The FT-IR and PXRD data of the reused and fresh **Pd(II)/COF-SDU1** were also consistent, which revealed the crystallinity and the atomic-level structure of **Pd(II)/COF-SDU1** were maintained (ESI, Fig. S4 and S5†).

Table 1 Recycle test of **Pd(II)/COF-SDU1** in one-pot silicon-based cross-coupling reaction of phenylsilane and 4-iodotoluene.

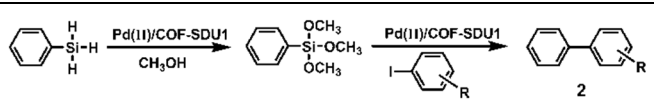


Entry	Catalyst	$t_1^a + t_2^b$ (h)	Yield (%) ^{c,d}
1	Fresh	10	96.5
2	Reused 1	10	95.1
3	Reused 2	12	94.6
4	Reused 3	10	95.3

Reaction conditions: ^a phenylsilane (1 mmol), methanol (5 mmol), **Pd(II)/COF-SDU1** (20 mg, 8.5×10^{-3} mmol of Pd) and THF (2 mL), room temperature, 3h. ^b 4-iodotoluene (1.1 mmol), TBAF (3 mmol), 80 °C, 7h. ^c Isolated yield. ^d The values are the average of two independent experiments.

The substrate generality under the same reaction conditions was also studied. Aryl iodide derivatives containing both electron-donating and electron-withdrawing groups were explored. As shown in Table 2, the coupling of aryl iodides containing the electron-withdrawing group (nitro and hydroxy) produced relatively lower efficiencies (66.5% and 68.5% yields, Table 2, entries 5–6). However, aryl iodides containing the electron-donating group such as methyl, methoxyl and fluoro coupled with organo(alkoxy)silanes well, gaining the corresponding products with good to excellent yields (91.4–96.5%, Table 2, entries 1–4). Additionally, 2-iodotoluene was also attempted to this reaction, which resulted in identically high yield with 4-iodotoluene, (Table 2, entry 2). In this way, the steric hindrance of iodobenzene derivatives could barely influence the reaction.

Table 2 Catalytic activity test of **Pd(II)/COF-SDU1** in one-pot silicon-based cross-coupling reaction of silanes and aryl iodides.



Entry	R	2	$t_1^a + t_2^b$ (h)	Yield (%) ^{c,d}
1	4-CH ₃	2a	10	96.5
2	2-CH ₃	2b	10	93.2
3	4-OCH ₃	2c	12	94.2
4	4-F	2d	10	91.4
5	4-OH	2e	16	68.5
6	4-NO ₂	2f	12	66.5

Reaction conditions: ^a phenylsilane (1 mmol), methanol (5 mmol), **Pd(II)/COF-SDU1** (20 mg, 8.5×10^{-3} mmol of Pd) and THF (2 mL), room temperature, 3h. ^b iodobenzene derivatives (1.1 mmol), TBAF (3 mmol), 80 °C, t_2 . ^c Isolated yield. ^d The values are the average of two independent experiments.

Conclusions

In summary, a new covalent organic framework (**COF-SDU1**) containing both imine and triazine functional groups was prepared. The as-obtained COF material possessed highly ordered crystalline structure and large surface area. Based on its stable, porous, nitrogen-rich properties, **COF-SDU1** can act as the efficient support for immobilizing and mono-dispersing Pd species. The **Pd(II)/COF-SDU1** showed superior performance in one-pot silicon-based cross-coupling reaction of silanes and aryl iodides with high selectivity. To the best of our knowledge, this is the first report to combine the oxidation of silanes and the next cross-coupling in one system by using COF/palladium hybrids as catalyst. Due to the particular structural properties of COFs materials incorporation with their easy functionalization to combine various metal, COF/metal hybrids will exhibit more future potential in catalytic field from both academia and industry.

Acknowledgements

Financial support from the Natural Science Foundation of China (Grant no. 21472117 and 21171106) is gratefully acknowledged.

Notes and references

^a Prof. Dr. X. Zhang

School of Chemistry and Chemical Engineering
Shandong University

27 South Shan Da Road, Jinan, Shandong 250100, China

E-mail: zhangxiaomei@sdu.edu.cn

^b Beijing Key Laboratory for Science and Application of Functional Molecular and Crystalline Materials, Department of Chemistry University of Science and Technology Beijing
Beijing, 100083, China.

† Electronic Supplementary Information (ESI) available: [Thermogravimetric analysis (TGA) data of **COF-SDU1** and **Pd(II)/COF-SDU1**; ¹³C CP/MAS NMR spectrum of trif; XPS spectrum of Pd(OAc)₂ and **Pd(II)/COF-SDU1**; PXRD patterns of **Pd(II)/COF-SDU1** before and after reused first and three times; Fourier transforms infrared (FT-IR) spectra of **Pd(II)/COF-SDU1** before and after reused first and three times in the region of 500–2000 cm⁻¹ with 2 cm⁻¹ resolution; Catalytic activity test of **Pd(II)/COF-SDU1** towards oxidation of organosilanes to organo(alkoxy)silanes or organosilanols; Catalytic activity test of **Pd(II)/COF-SDU1** towards silicon-based cross-coupling reaction of the organo(alkoxy)silanes or organosilanols with aryl iodides]. See DOI: 10.1039/b000000x/

- 1 L. Yin and J. Liebscher, *Chem. Rev.*, 2007, **107**, 133–173.
- 2 Y. Nakao and T. Hiyama, *Chem. Soc. Rev.*, 2011, **40**, 4893–4901.
- 3 S.E. Denmark and M.H. Ober, *Aldrichim. Acta*, 2003, **36**, 75–85.
- 4 (a) K. Valliant-Saunders, E. Gunn, G. Shelton, D. Hrovat, W. Borden and J. Mayer, *Inorg. Chem.*, 2007, **46**, 5212–5219. (b) P. D. Lickiss and R. Lucas, *J. Organomet. Chem.*, 1996, **521**, 229–234. (c) L. Spialter and J. Austin, *J. Am. Chem. Soc.*, 1965, **87**, 4406–4406. (d) L.

- Sommer, L. Ulland and G. Parker, *J. Am. Chem. Soc.*, 1972, **94**, 3469-3471.
- 5 (a) R. Ishimoto, K. Kamata and N. Mizuno, *Angew. Chem. Int. Ed.*, 2009, **48**, 8900-8904; (b) T. Mitsudome, A. Noujima, T. Mizugaki, K. Jitsukawa and K. Kaneda, *Chem. Commun.*, 2009, 5302-5304.
- 6 Z. Li, S. Lin, L. Ji, Z. Zhang, X. Zhang and Y. Ding, *Catal. Sci. Technol.*, 2014, **4**, 1734-1737.
- 7 (a) X. Liu, C. Guan, D. Wang and L. Wan, *Adv. Mater.*, 2014, **26**, 6912-6920; (b) S. Ding and W. Wang, *Chem. Soc. Rev.*, 2013, **42**, 548-568; (c) X. Feng, X. Ding and D. Jiang, *Chem. Soc. Rev.*, 2012, **41**, 6010-6022.
- 8 (a) S. B. Kalidindi, H. Oh, M. Hirscher, D. Esken, C. Wiktor, S. Turner, G. V. Tendeloo and R. A. Fischer, *Chem. Eur. J.*, 2012, **18**, 10848-10856; (b) S. B. Kalidindi and R. A. Fischer, *Phys. Status Solidi B*, 2013, **250**, 1119-1127; (c) Z. Li, X. Feng, Y. Zou, Y. Zhang, H. Xia, X. Liu and Y. Mu, *Chem. Commun.*, 2014, **50**, 13825-13828; (d) M. G. Rabbani, A. K. Sekizkardes, Z. Kahveci, T. E. Reich, R. Ding and H. M. El-Kaderi, *Chem. Eur. J.*, 2013, **19**, 3324-3328.
- 9 (a) S. Wan, J. Guo, J. Kim, H. Ihee and D. Jiang, *Angew. Chem. Int. Ed.*, 2008, **47**, 8826-8830; (b) S. Wan, J. Guo, J. Kim, H. Ihee and D. Jiang, *Angew. Chem. Int. Ed.*, 2009, **48**, 5439-5442; (c) X. Ding, L. Chen, Y. Honsho, X. Feng, O. Saenpawang, J. Guo, A. Saeki, S. Seki, S. Irle, S. Nagase, V. Parasuk and D. Jiang, *J. Am. Chem. Soc.*, 2011, **133**, 14510-14513.
- 10 (a) S. Ding, J. Gao, Q. Wang, Y. Zhang, W. Song, C. Su and W. Wang, *J. Am. Chem. Soc.*, 2011, **133**, 19816-19822; (b) P. Pachfule, S. Kandambeth, D. D. Diaz and R. Banerjee, *Chem. Commun.*, 2014, **50**, 3169-3172; (c) P. Pachfule, M. K. Panda, S. Kandambeth, S. M. Shivaprasad, D. D. Diaz and R. Banerjee, *J. Mater. Chem. A*, 2014, **2**, 7944-7952; (d) C. E. Chan-Thaw, A. Villa, L. Prati and A. Thomas, *Chem. Eur. J.*, 2011, **17**, 1052-1057; (e) R. Palkovits, M. Antonietti, P. Kuhn, A. Thomas and F. Schüth, *Angew. Chem. Int. Ed.*, 2009, **48**, 6909-6912; (f) J. Artz, S. Mallmann and R. Palkovits, *ChemSusChem*, DOI: 10.1002/cssc.201403078; (g) J. Roeser, K. Kailasam and A. Thomas, *ChemSusChem*, 2012, **5**, 1793-1799; (h) L. Stegbauer, K. Schwinghammer and B. V. Lotsch, *Chem. Sci.*, 2014, **5**, 2789-2793.
- 11 P. Zhang, Z. Weng, J. Guo and C. Wang, *Chem. Mater.*, 2011, **23**, 5243-5249.
- 12 C. E. Chan-Thaw, A. Villa, P. Katekomol, D. Su, A. Thomas and L. Prati, *Nano Lett.*, 2010, **10**, 537-541.
- 13 H. L. Jiang, T. Akita, T. Ishida, M. Haruta and Q. Xu, *J. Am. Chem. Soc.*, 2011, **133**, 1304-1306.
- 14 (a) B. Crozon, M. Besson and P. Gallezot, *New J. Chem.*, 1998, **22**, 269-273; (b) T. Mallat and A. Baiker, *Catal. Today*, 1994, **19**, 247-284; (c) P. Vinke, D. deWit, A. T. J. W. de Goede and H. van Bekkum, *New Developments in Selective Oxidation by Heterogeneous Catalysis, Studies in Surface Science and Catalysis*, Vol. 72, Elsevier, Amsterdam, 1992, pp. 1-20; (d) P. Gallezot, *Catal. Today*, 1997, **37**, 405-418.
- 15 F. Yang, J. Xie, H. Guo, B. Xu and C. Li, *Liquid Crystals*, 2012, **39**, 1368-1374.
- 16 (a) Y. M. A. Yamada, S. M. Sarkar and Y. Uozumi, *J. Am. Chem. Soc.*, 2012, **134**, 3190-3198; (b) H. Li, Z. Zhu, F. Zhang, S. Xie, H. Li, P. Li and X. Zhou, *ACS Catal.*, 2011, **1**, 1604-1612.
- 17 S. Wan, F. Gándara, A. Asano, H. Furukawa, A. Saeki, S. K. Dey, L. Liao, M. W. Ambrogio, Y. Y. Botros, X. Duan, S. Seki, J. F. Stoddart and O. M. Yaghi, *Chem. Mater.*, 2011, **23**, 4094-4097.
- 18 R. Wahl, M. Mertig, J. Raff, S. Selenska-Pobell and W. Pompe, *Adv. Mater.*, 2001, **13**, 736-740.
- 19 (a) F. J. Uribo-Romo, C. J. Doonan, H. Furukawa, K. Oisaki and O. M. Yaghi, *J. Am. Chem. Soc.*, 2011, **133**, 11478-11481; (b) M. Dogru, M. Handloser, F. Auras, T. Kunz, D. Medina, A. Hartschuh, P. Knochel and T. Bein, *Angew. Chem. Int. Ed.*, 2013, **52**, 2920-2924.
- 20 P. Kuhn, M. Antonietti and A. Thomas, *Angew. Chem. Int. Ed.*, 2008, **47**, 3450-3453.
- 21 (a) K. T. Jackson, T. E. Reich and H. M. El-Kaderi, *Chem. Commun.*, 2012, **48**, 8823-8825; (b) B. Lukose, A. Kuc and T. Heine, *Chem. Eur. J.*, 2011, **17**, 2388-2392.
- 22 N. T. Tran, S. O. Wilson and A. K. Franz, *Org. Lett.*, 2012, **14**, 186-189.